Local velocity scaling in upward flow to tooth impeller in a fully turbulent region

Radek Šulc[1,*], *Pavel* Ditl[1], *Ivan* Fořt[1], *Darina* Jašíkova[2], *Michal* Kotek[2], *Václav* Kopecký[2], and *Bohuš* Kysela[3]

[1]Czech Technical University in Prague, Faculty of Mechanical Engineering, Department of Process Engineering, Technická 4, 166 07 Prague, Czech Republic
[2]Technical University of Liberec, Institute for Nanomaterials, Advanced Technology and Innovation, Studentská 1402/2, 461 17 Liberec, Czech Republic
[3]Czech Academy of Sciences, Institute of Hydrodynamics v.v.i, Pod Pat'ankou 30/5, 166 12 Prague, Czech Republic

Abstract. The hydrodynamics and flow field were measured in an agitated vessel using 2-D Time Resolved Particle Image Velocimetry (2-D TR PIV). The experiments were carried out in a fully baffled cylindrical flat bottom vessel 400 mm in inner diameter agitated by a tooth impeller 133 mm in diameter. Distilled water was used as the agitated liquid. The velocity fields were investigated in the upward flow to the impeller for three impeller rotation speeds – 300 rpm, 500 rpm and 700 rpm, corresponding to a Reynolds number in the range 94 000 < Re < 221 000. This means that fully-developed turbulent flow was reached. This Re range secures the fully-developed turbulent flow in an agitated liquid. In accordance with the theory of mixing, the dimensionless mean and fluctuation velocities in the measured directions were found to be constant and independent of the impeller Reynolds number. On the basis of the test results the spatial distributions of dimensionless velocities were calculated. The axial turbulence intensity was found to be in the majority in the range from 0.4 to 0.7, which corresponds to the middle level of turbulence intensity.

1 Introduction

It is important to know the flow and the flow pattern in an agitated vessel in order to determine many impeller and turbulence characteristics, e.g. impeller pumping capacity, intensity of turbulence, turbulent kinetic energy, convective velocity, and the turbulent energy dissipation rate. The information and data that are obtained can also be used for CFD verification.

In PIV studies, the spatial distributions of various properties are often presented. However, the inspection analysis shows that the validity of the spatial distribution of any dimensionless property for arbitrary process conditions in geometrically similar agitated vessels requires independence of a given dimensionless property from the impeller Reynolds number. The spatial distribution that is obtained is in general valid only when this independence is both theoretically predicted and experimentally verified. Unfortunately, in many studies the results are presented only for one impeller speed and, in addition the experiments are often carried out in the transient flow regime.

Agitation of two immiscible liquids or solid-liquid suspension is a frequent operation in chemical and metallurgical industries. In this case the tooth impeller has been used usually for dispersion process.

In our previous work [1] the scaling of the velocity field in the zone in upward flow to the impeller for three liquids of different viscosities in a vessel 400 mm in the inner diameter agitated by a tooth impeller were presented.

The aim of this work is to study scaling of the velocity field in the upward flow to the impeller in a vessel 400 mm in inner diameter mechanically agitated by a tooth impeller (CVS 691038.1) in a fully turbulent region. The independency of dimensionless spatial velocity distribution on the impeller Reynolds number was tested statistically. The hydrodynamics and the flow field were measured in an agitated vessel using Time Resolved Particle Image Velocimetry (TR PIV).

2 Theoretical background

2.1 Inspection analysis of flow in an agitated vessel

The flow of a Newtonian fluid in an agitated vessel has been described by the Navier – Stokes equation:

$$\rho \cdot \left(\frac{\partial \vec{U}}{\partial t} + \vec{U} \bullet \nabla \vec{U} \right) = -\nabla p + \mu \cdot \nabla^2 \vec{U} + \rho \cdot \vec{g} \qquad (1)$$

This equation can be rewritten into dimensionless form, as follows (e.g. [2]):

* Corresponding author: radek.sulc@fs.cvut.cz

$$\left(\frac{\partial \vec{U}^*}{\partial t^*} + \vec{U}^* \bullet \nabla^* \vec{U}^*\right) = -\nabla^* p^* + \frac{1}{\mathrm{Re}} \cdot \nabla^{*2} \vec{U}^* + \frac{1}{Fr} \cdot \vec{n}^* \quad (2)$$

where the dimensionless properties are defined as follows:

- dimensionless instantaneous velocity:

$$\vec{U}^* = \frac{\vec{U}}{N \cdot D}, \quad (3a)$$

- dimensionless instantaneous pressure:

$$p^* = \frac{p}{\rho \cdot N^2 \cdot D^2}, \quad (3b)$$

- dimensionless space gradient: $\nabla^* = \frac{\nabla}{D}$, (3c)

- impeller Reynolds number $\mathrm{Re} = \frac{N \cdot D^2}{\nu}$, (3d)

- impeller Froude number: $Fr = \frac{N^2 \cdot D}{g}$, (3e)

and where $\vec{n}$ is a unity vector.

Similarly, the equation of continuity for stationary flow of a non-compressible fluid is given

$$\nabla \bullet \vec{U} = 0 \quad (4)$$

and one can be rewritten into the dimensionless form as follows:

$$\nabla^* \bullet \vec{U}^* = 0 \quad (5)$$

The following relations can be obtained for the dimensionless velocity components and the dimensionless pressure, respectively, by inspection analysis of Eqs. (2) and (5), as follows:

$$\vec{U}^* = f_1(\vec{x}^*, t^*, \mathrm{Re}, Fr), \quad (6)$$

$$p^* = f_2(\vec{x}^*, t^*, \mathrm{Re}, Fr), \quad (7)$$

where $\vec{x}^*$ is a dimensionless location vector.

For stationary flow with a periodic character the velocity time dependence can be eliminated by substituting the velocity and pressure by time-averaged properties. For highly turbulent flow in a baffled vessel, the viscous and gravitational forces can be neglected and finally the time-averaged dimensionless velocity components and the pressure are independent of the impeller Reynolds and the Froude numbers, and depend on location only:

$$\overline{U}_i^* = f_1(\vec{x}^*), \quad (8)$$

$$p^* = f_2(\vec{x}^*). \quad (9)$$

Reynolds decomposition of instantaneous velocity components has been applied for the velocity profiles studied in this work.

2.2 Mean and fluctuation velocity

Using PIV, the instantaneous velocity data set U_i (t_j) in the ith direction for j = 1, 2, … N_R at observation times t_j with equidistant time step Δt_S (i.e. $\Delta t_S = t_{j+1} - t_j$) was obtained in a given location. Assuming the ergodic hypothesis the time-averaged mean velocity $\overline{U}_i$ was determined as the average value of velocity data set U_i (t_j):

$$\overline{U}_i = \frac{1}{N_R} \cdot \sum_j U(t_j) \quad \text{for } j = 1, 2, \ldots, N_R, \quad (10)$$

where $\overline{U}_i$ is mean velocity in the ith direction, U_i (t_j) is instantaneous velocity in the ith direction at the observation time t_j, and N_R is the number of data items in the velocity data set.

Consequently, the fluctuation velocity in the ith direction u_i (t_j) at observation time t_j is obtained by decomposition of the instantaneous velocity:

$$u_i(t_j) = U_i(t_j) - \overline{U}_i \quad \text{for } j = 1, 2, \ldots, N_R, \quad (11)$$

where u_i (t_j) is the fluctuation velocity in the ith direction at observation time t_i, $\overline{U}_i$ is mean velocity in the ith direction, U_i (t_i) is instantaneous velocity in the ith direction at the observation time t_i.

The root mean squared fluctuation velocity is determined as follows:

$$\overline{u}_i = \left(\frac{1}{N_R} \cdot \sum_i u_i^2(t_j)\right)^{1/2} \quad \text{for } j = 1, 2, \ldots, \mathrm{N_R}, \quad (12)$$

where $\overline{u}_i$ is the root mean squared fluctuation velocity, and u (t_i) is the fluctuation velocity at observation time t_i.

3 Experimental

The hydrodynamics and the flow field were investigated in an agitated vessel using Time Resolved Particle Image Velocimetry (TR PIV). The experiments were carried out in a fully baffled cylindrical flat bottom vessel 400 mm in the inner diameter. The tank was agitated by a tooth impeller 133 mm in diameter, i.e. the dimensionless impeller diameter *D/T* was 1/3. The dimensionless impeller clearance *C/D* taken from the lower impeller edge was 0.75. The tank was filled with degassed liquid, and the liquid height was 400 mm, i.e. the dimensionless liquid height *H/T* was 1. The dimensionless baffle width *B/T* was 1/10. To prevent air suction the vessel was covered by a lid. The distilled water (ν = 9.35x10^{-7} m^2/s) was used as the agitated liquid.

Table 1. Operational parameters.

Run #	liquid	N (rpm)	ν (m^2/s)	Re (-)	Record time T_R (s)
w-N300	water	300	9.35×10^{-7}	94 641	16
w-N500	water	500	9.35×10^{-7}	157 735	16
w-N700	water	700	9.35×10^{-7}	220 829	16

The velocity fields were measured at an impeller rotation speed in the range from 300 rpm to 700 rpm, which covers the impeller Reynolds number range from 94 000 to 221 000. This Re range secures the fully-developed turbulent flow. The operational conditions are summarized in Table 1.

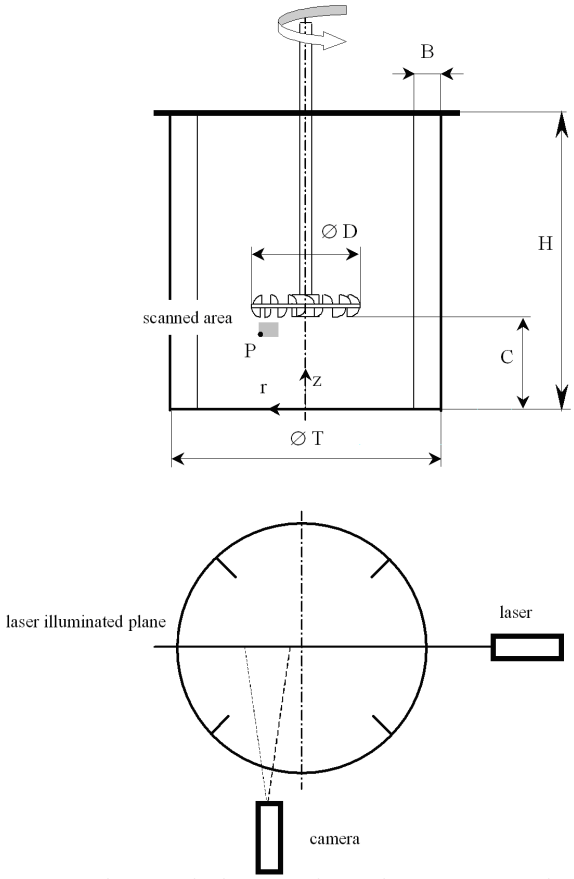

Fig. 1. Scheme of the experimental apparatus and the investigated area.

The time-resolved LITRON LDY 302 2D-PIV system (Dantec Dynamics (Denmark)) consists of a Neodyme-YLF laser (light wave length 532 nm, impulse energy 2x15 mJ), a SpeedSence 611 high speed PIV-regime camera (working on frequency 1kHz with resolution 1280 x 800 pixels) with a Nikon Macro 200 optical lens system equipped with an optical filter of wave length 570 nm. Rhodamine B fluorescent particles 11.95 ± 0.25 μm in mean diameter were used as seeding particles. The fluorescent particles lit by 532 nm light emit 570 nm light. In this way, non-seeding particles such as impurities and bubbles are separated, and are not recorded. The operating frame rate was 1 kHz (1000 vector fields per second), i.e. the sampling time Δt_s was 1 ms. The measured vertical plane was located in the center of the vessel and in the middle of the baffles. The plane was illuminated by a laser sheet. The investigated area was 25.6 x 16 mm, and the PIV spatial resolution Δ = 0.64 mm was maintained the same during the experiment.

The position of left bottom apex P [r_P; z_P] was [57.8; 47], i.e. dimensionless radius $2r/T$ = 0.289 and dimensionless height z/T = 0.1175. The scheme of the experimental apparatus and the investigated area is depicted in Fig. 1. The camera was positioned orthogonally to the laser sheet. The investigated area corresponds to region O according to the classification given by Fořt et al. [3].

4 Experimental data evaluation

According to the inspection analysis, the dimensionless velocities normalized by the product of impeller speed N and impeller diameter D should be independent of the impeller Reynolds number.

The effect of impeller Reynolds number on dimensionless velocities was tested by hypothesis testing ([6]). The statistical method of hypothesis testing can estimate whether the differences between the predicted parameter values (e.g. according to some proposed theory) and then the parameter values evaluated from the measured data are negligible. In this case, we assumed dependence of the tested parameter on the impeller Reynolds number, described by the simple power law correlation $parameter = B.Re^{\beta}$, and the difference between predicted exponent β_{pred} and evaluated exponent β_{calc} was tested. The hypothesis test characteristics are given as $t = (\beta_{calc} - \beta_{pred})/ s_\beta$ where s_β is the standard error of parameter β_{calc}. If the calculated $|t|$ value is less than the critical value of the t-distribution for (m-2) degrees of freedom and significance level α, the difference between β_{calc} and β_{pred} is statistically negligible (statisticians state: "the hypothesis cannot be rejected"). In our case, the independence of dimensionless velocities of the impeller Reynolds number was tested as the hypothesis, i.e. $parameter = B.(Re)^0$ = const., i.e. β_{pred} = 0. The t-distribution coefficient $t_{(m-2),\ \alpha}$ for three impeller Reynolds numbers and significance level α = 0.05 is 12.706. The hypothesis testing was done for each point in the investigated area. The hypothesis test results are presented for investigated area in Table 2 by the percentage of points in which the above-formulated hypothesis *parameter = const.* is satisfied and by the percentage of points in which the hypothesis parameter = const. can not be accepted.

Table 2. Dimensionless velocities – effect of the impeller Reynolds number

	Hypothesis: parameter = B.(Re)^0 percentage / t-characteristics |t|	
Parameter	acceptable	not acceptable
$\overline{U}_r/(ND)$ (-)	99.3 % / 3.3	0.7 % / 13.9
$\overline{U}_{ax}/(ND)$ (-)	98.2 % / 1.72	1.8 % / 46
$\overline{u}_r/(ND)$ (-)	100 % / 0.38	0 % / 0
$\overline{u}_{ax}/(ND)$	85.1 % / 4.87	14.9 % / 72
T.I.$_r$ (-)	98.6 % / 3.74	1.4 % / 47
T.I.$_{ax}$ (-)	92.8 % / 3.33	7.2 % / 49

For illustration, the average values of calculated $|t|$ value are presented here also.

The dimensionless axial mean velocities were found in the range from 0.075 to 0.22. The dimensionless radial mean velocities were found to be close to zero, in the range from 0.048 to 0.088. These findings correspond to characteristics of the given zone, according to Fořt et al. [3]. This region contains predominantly axial flow to the impeller. The dimensionless radial mean velocities are lower than the dimensionless values for axial mean velocity as expected for this region. The tested hypothesis can be accepted in the majority of profile points of the investigated area.

The dimensionless radial r.m.s. fluctuation velocities were found to be in the range from 0.070 to 0.106. The tested hypothesis can be accepted in the all profile points, as is signalized by the lowest calculated $|t|$ values.

The dimensionless axial r.m.s. fluctuation velocities were found to be in the range from 0.061 to 0.086. The tested hypothesis can be accepted in the relatively high number of profile points.

On the basis of the results of this hypothesis test, we assume that all dimensionless velocities can be statistically taken as constant and independent of the impeller Reynolds number. The spatial distributions of dimensionless velocities for seven operational conditions were averaged and are presented in Figures 2 – 5. For illustration, the radial profiles of velocity components are presented in Figures 6 - 9 for selected axial positions $z^* = 0.125$, 0.137 and 0.150.

Intensity of turbulence

The radial and axial turbulence intensity were calculated for each point in the investigated area as follows:

$$T.I._i = \frac{\overline{u}_i}{\overline{U}_i} \tag{13}$$

where $\overline{u}_i$ and $\overline{U}_i$ are r.m.s. fluctuation velocity and mean velocity respectively in given direction. For dimensionless velocities independent of the impeller Reynolds number, the turbulence intensity should also be independent of this quantity. The independence of intensities of turbulence from the impeller Reynolds number was again tested by hypothesis testing. The t-distribution coefficient $t_{(m-2),\ \alpha}$ for three impeller Reynolds numbers and significance level $\alpha = 0.05$ is 12.706. Hypothesis testing was done for each point in the investigated area. The hypothesis test results are presented in Table 2, as well.

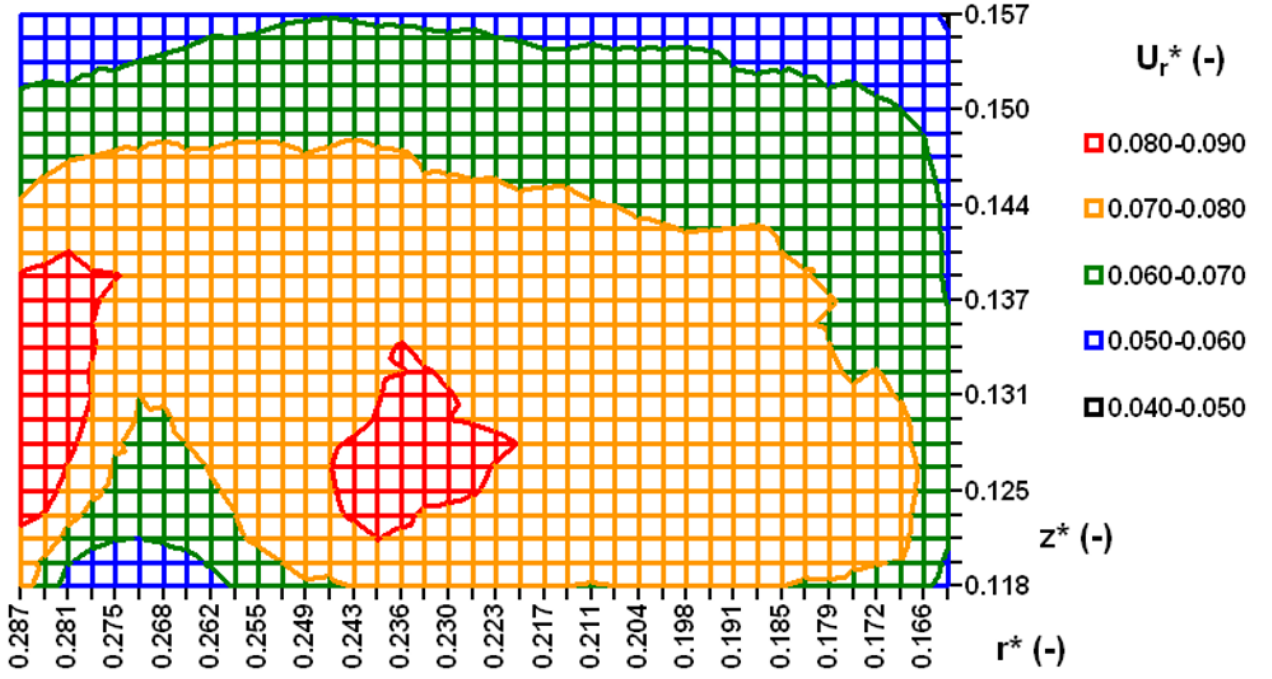

Fig. 2. Dimensionless radial mean velocity distribution $U_r^* = \overline{U}_r/(ND) = f(r^*, z^*)$.

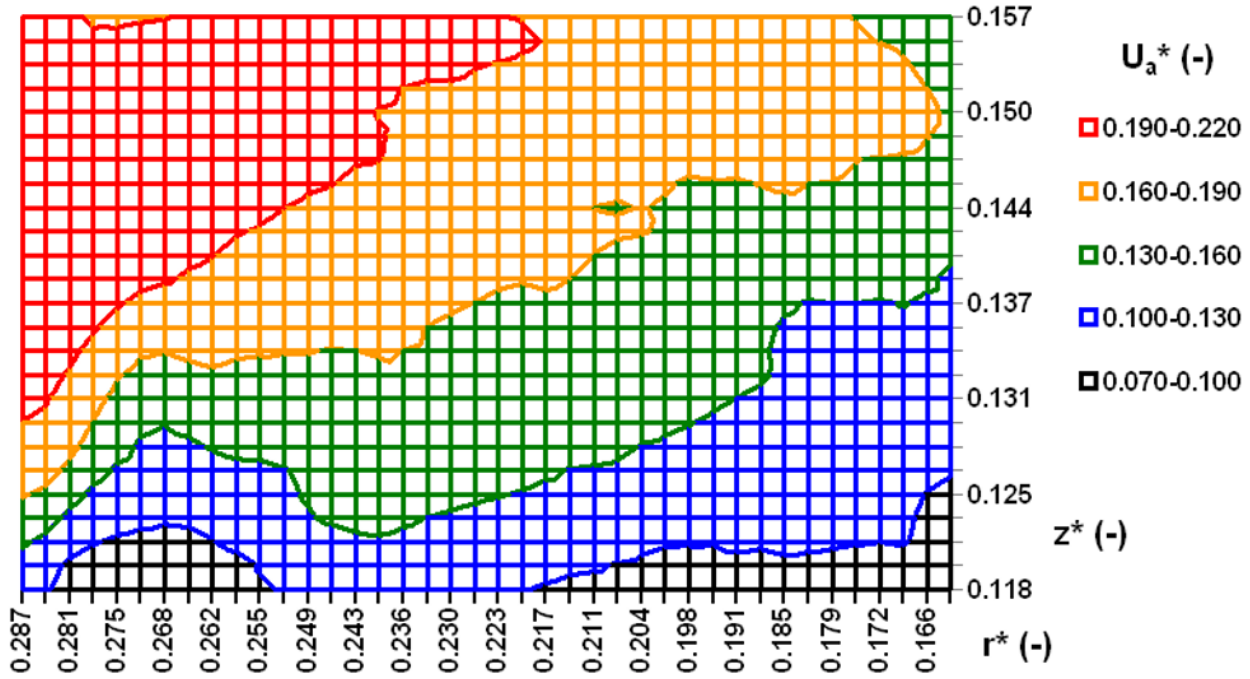

Fig. 3. Dimensionless axial mean velocity distribution $U_{ax}^{*} = \overline{U}_{ax}/(ND) = \mathrm{f}(r^{*}, z^{*})$.

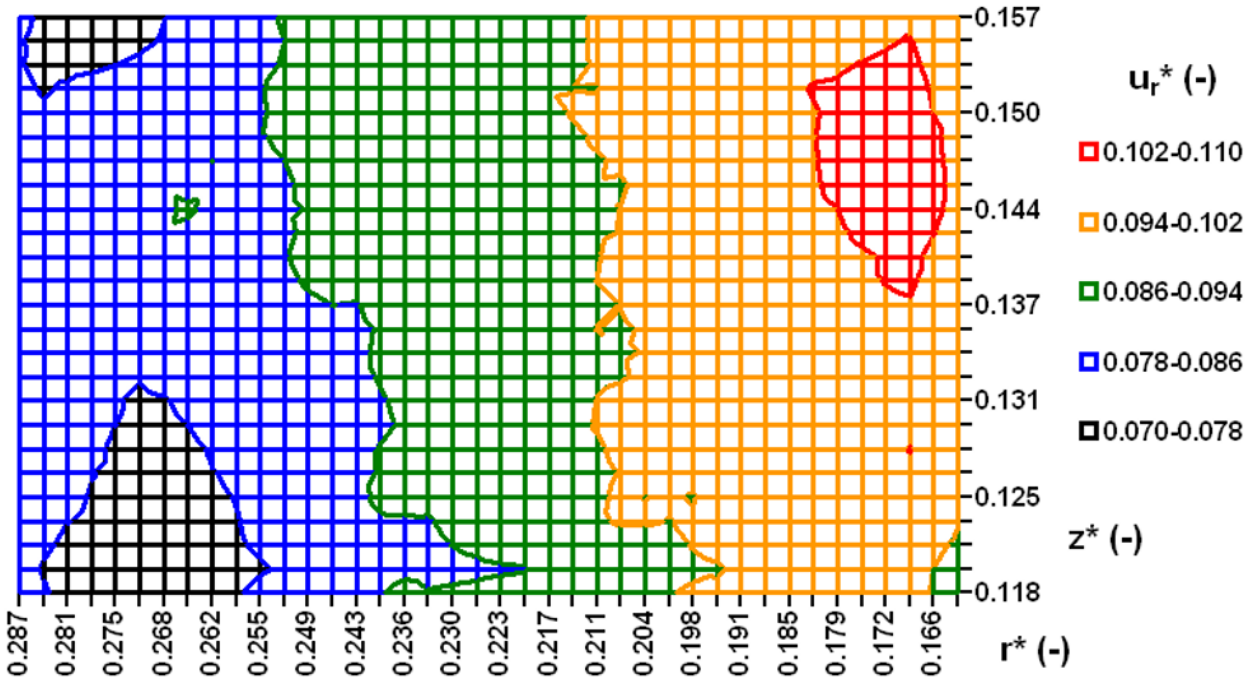

Fig. 4. Dimensionless radial fluctuation velocity distribution $u_r^{*} = \overline{u}_r/(ND) = \mathrm{f}(r^{*}, z^{*})$.

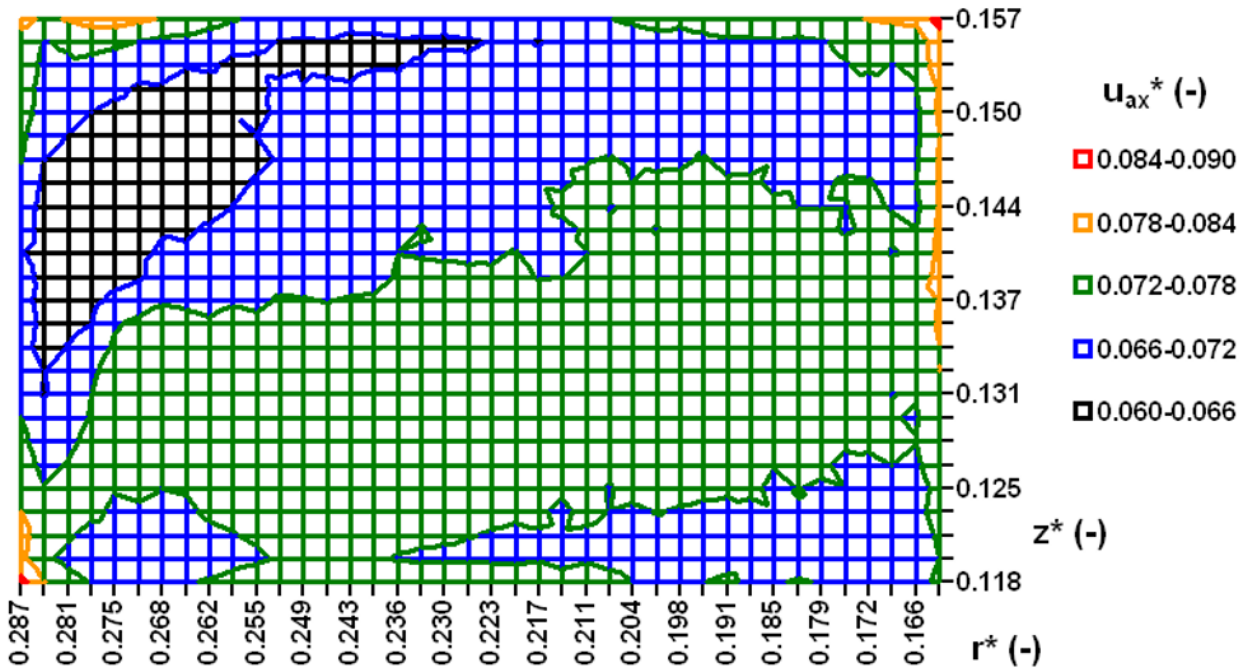

Fig. 5. Dimensionless axial fluctuation velocity distribution $u_{ax}^{*} = \overline{u}_{ax}/(ND) = \mathrm{f}(r^{*}, z^{*})$.

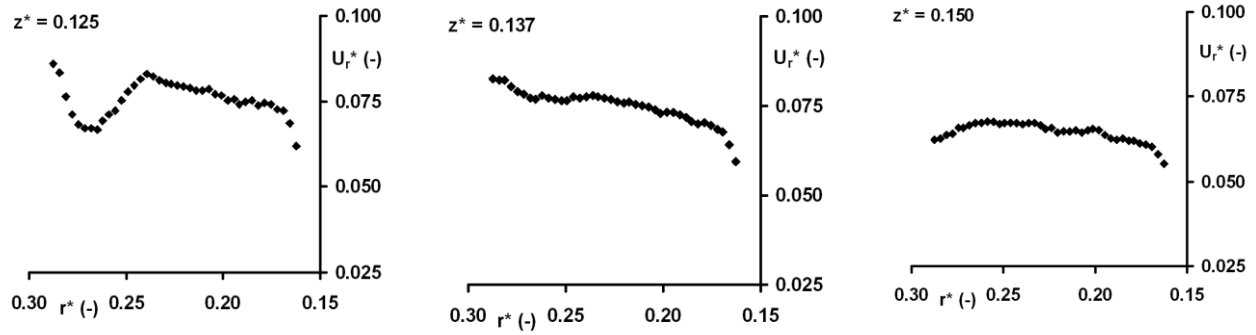

Fig. 6. Dimensionless radial mean velocity profiles $\overline{U}_{r}/(ND) = \mathrm{f}(\mathrm{r}^{*})$.

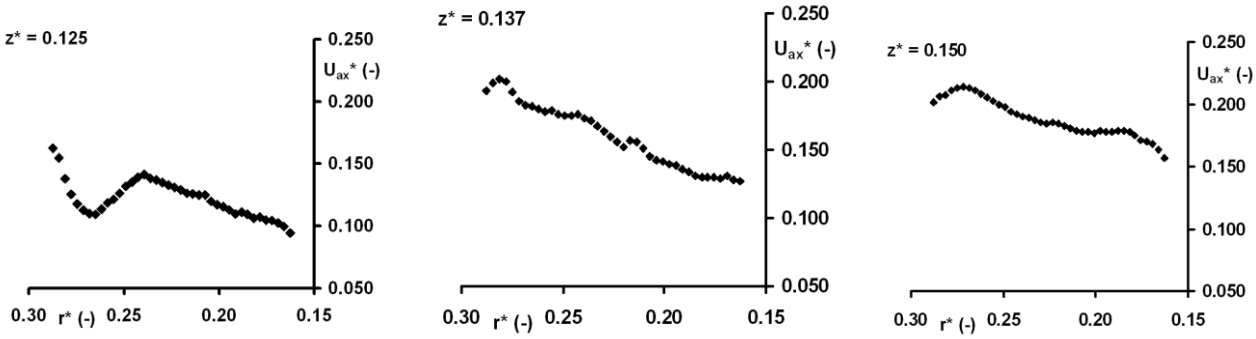

Fig. 7. Dimensionless axial mean velocity profiles $\overline{U}_{ax}/(ND) = \mathrm{f}(r^{*})$.

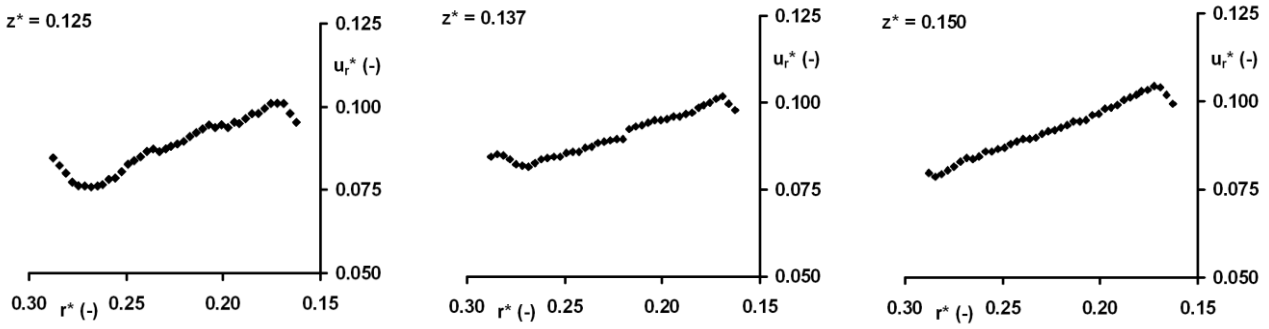

Fig. 8. Dimensionless radial fluctuation velocity profiles $\overline{u}_r /(ND) = \mathrm{f}(r^*)$.

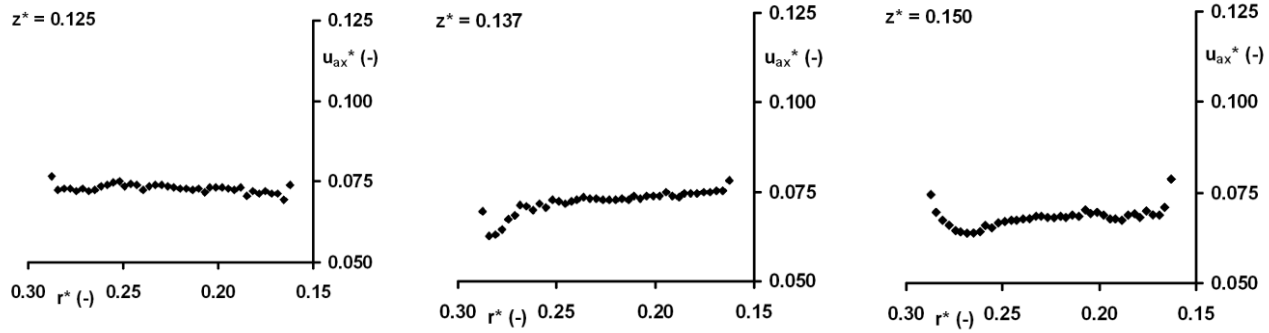

Fig. 9. Dimensionless axial fluctuation velocity profiles $\overline{u}_{ax} /(ND) = \mathrm{f}(r^*)$.

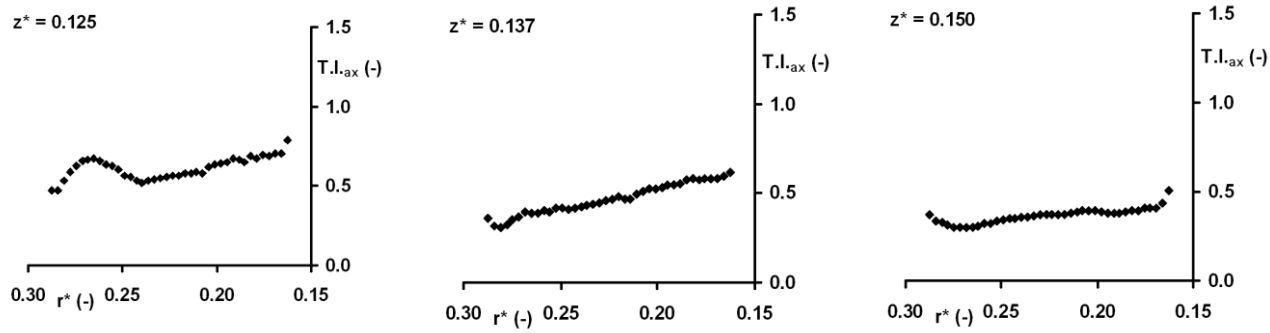

Fig. 10. Axial turbulence intensity profiles $T.I._{ax} = \mathrm{f}(r^*)$.

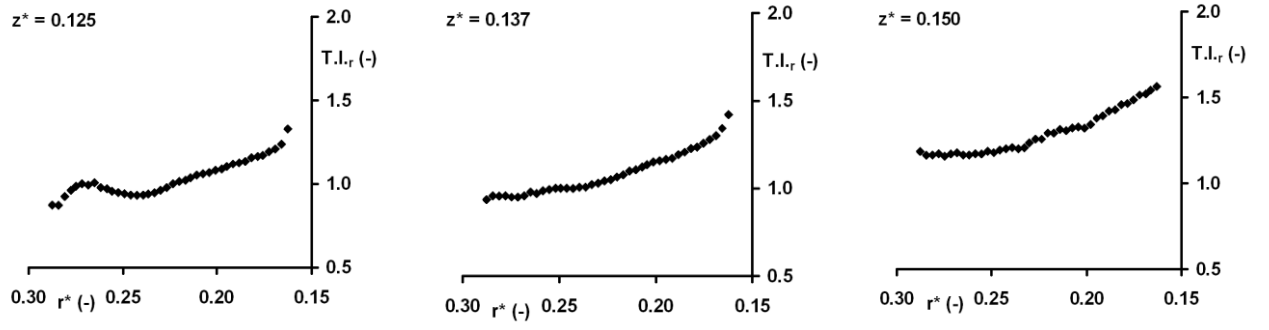

Fig. 11. Radial turbulence intensity profiles $T.I._r = \mathrm{f}(r^*)$.

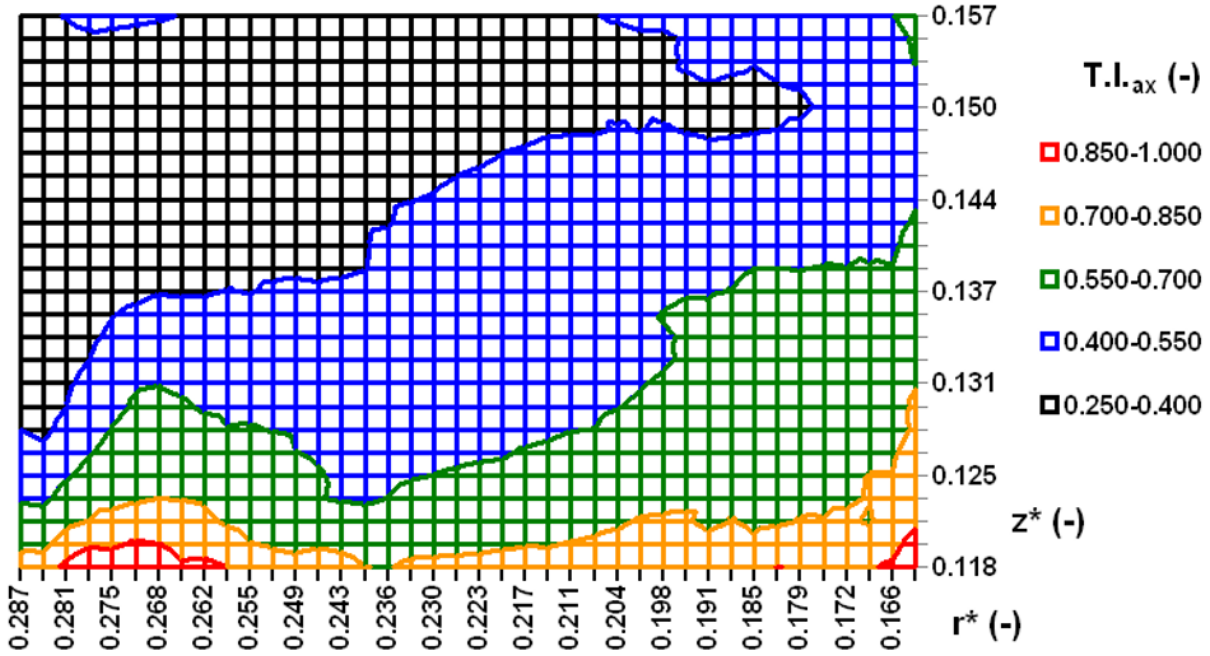

Fig. 12. Axial turbulence intensity distribution $T.I._{ax} = \mathrm{f}(r^*, z^*)$.

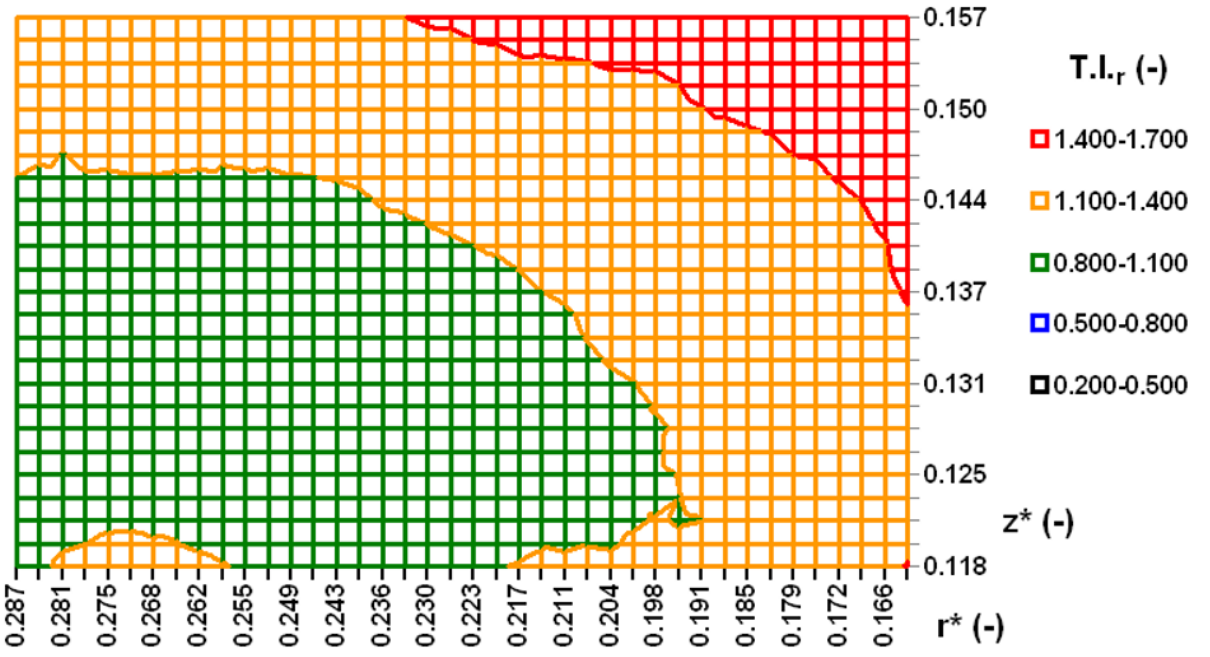

Fig. 13. Radial turbulence intensity distribution $T.I._r = \mathrm{f}(r^*, z^*)$.

The tested hypothesis can be accepted in the majority of profile points. On the basis of these hypothesis test results, we assume that both radial and axial turbulence intensity can be statistically taken as constant and independent of the impeller Reynolds number, as expected. Owing to the selected position that is relatively far from the impeller and outside of the impeller discharge flow, we expected low turbulence intensity. This expectation was not confirmed. As shown, the calculated values of radial turbulence intensity are in the majority of points in the range from 0.8 to 1.4. These values correspond to high turbulence intensity. The calculated values of axial turbulence intensity are in the majority of points in the range from 0.4 to 0.7. These values correspond to middle turbulence intensity. The radial mean and fluctuation velocities in the upward flow are approx. 11÷20 and 4÷6 times lower respectively comparing with the radial mean and fluctuation velocities in the impeller discharge flow. The axial mean and fluctuation velocities in the upward flow are approx.

2÷10 times higher and 5÷7 times lower respectively comparing with the axial mean and fluctuation velocities in the impeller discharge flow [1]. Therefore, the values of turbulence intensity are higher than we expected. The radial profiles of axial and radial turbulence intensities are presented in Figures 10 and 11 respectively for selected axial positions $z^* = 0.125$, 0.137 and 0.150. The spatial distribution of quantities $T.I._{ax}$ and $T.I._r$ are shown in Figures 12 and 13 respectively.

5 Conclusions

The following results have been obtained in this study:

The hydrodynamics and flow field were measured in a vessel 400 mm in the inner diameter agitated by a tooth impeller using the 2-D Time Resolved Particle Image Velocimetry (2-D TR PIV). Distilled water was used as the agitated liquid. The velocity fields were measured in the upward flow to the impeller for impeller rotation speeds from 300 rpm to 700 rpm corresponding to the impeller Reynolds number in the range 94 000 < Re < 221 000.

The dimensionless radial mean velocities were found to be close to zero. These findings correspond to the characteristics of the given zone according to Fořt et al. [3]. This region contains predominantly axial flow to the impeller.

In accordance with the theory of mixing, the dimensionless mean and fluctuation velocities in measured directions were found to be constant and independent of the impeller Reynolds number. On the basis of the test results the spatial distributions of dimensionless velocities were calculated.

The axial turbulence intensity was calculated and was found to be in the majority of points in the range from 0.4 to 0.7, which corresponds to middle level of turbulence intensity. Unlike this, the radial turbulence was found to be igher values comparing with axial turbulence intensity. The values of radial turbulence intensity were in the range from 0.8 to 1.4 in the majority of points, which corresponds to high level of turbulence intensity. It was found that the both radial and axial turbulence intensities can be statistically taken as constant and independent of the impeller Reynolds number.

This research has been supported by Grant Agency of the Czech Republic project No. 16-20175S and by Ministry of Education, Youth and Sports of the Czech Republic project No. LO1201 (National Programme for Sustainability I) and RVO:67985874.

Symbols

B baffle width, m
C impeller clearance, m
D impeller diameter, m
H liquid height, m
m number of experimental points, -
N impeller rotational speed, 1/s
N_R number of data in velocity data set, -
r radius (radial coordinate), m
r^* dimensionless radius; $r^* = 2r/T$, -
Re impeller Reynolds number; $Re = N.D^2/\nu$, -
t time, s
t_i observation time, s
t_R record time, s
$t_{(m-2),\ a=0.05}$ t-distribution for (m-2) degrees of freedom and significance level α, -
T tank diameter, m
T.I. turbulence intensity, -
u_i fluctuation velocity in i^{th} direction, m/s
$\overline{u_i}$ root mean squared fluctuation velocity in i^{th} direction, m/s
U_i instantaneous velocity in i^{th} direction, m/s
$\overline{U_i}$ mean velocity in i^{th} direction, m/s
z actual height (axial coordinate), m
z^* dimensionless height; $z^* = z/T$, -

References

1. R. Šulc, P. Ditl, I. Fořt, D. Jašíková, M. Kotek, V. Kopecký, B. Kysela, Local velocity scaling in an impeller discharge flow in T400 vessel agitated by tooth impeller in a fully turbulent region. EPJ Web Conf., **180**, Article No. 02102 (2018)
2. V. Novák, F. Rieger, K. Vavro, *Hydraulické pochody v chemickém a potravinářském průmyslu* (SNTL, Prague, 1989)
3. I. Fořt, A. Obeid, V. Březina, Coll. Czechoslov. Chem. Comm., **47**, 226-239 (1982)
4. B.L. Bowerman, R.T.O´Connell, *Applied statistics: improving business processes* (Richard D. Irwin, USA, 1997)